

# Effects of Selected Roofing Materials and Angle of Incidence on Nav aids Signal Strength

\*Robert J. Omusonga

Directorate of Air Navigation Services, East African School of Aviation  
P.O Box 93939-80100, Mombasa, Kenya  
Email: [romusonga@gmail.com](mailto:romusonga@gmail.com)

Daudi M. Nyaanga

Department of Agricultural Engineering, Egerton University  
P.O Box 536-20115, Egerton, Kenya  
Email: [dmnyaanga@gmail.com](mailto:dmnyaanga@gmail.com)

Jason M. Githeko

Department of Computer Science, Egerton University  
P.O Box 536-20115, Egerton, Kenya  
Email: [githeko@gmail.com](mailto:githeko@gmail.com)

Boniface K. Chomba

Department of Information and Telecommunication Engineering, Technical University of Kenya  
P.O Box 52428-00200, Nairobi, Kenya  
Email: [bchomba08@gmail.com](mailto:bchomba08@gmail.com)

## Abstract

Interference that causes partial loss of intelligence in air navigation signal is largely dependent on the environment around radio navigation aids (nav aids). Buildings around airports have been restricted partly because they pose a technical threat to flight navigation. Previous studies have shown that about 50% of air accidents occur during landing. However no data has been availed to determine the contribution of nav aids to these accidents. The purpose of this paper was to determine the effects of roofing materials on air navigation signal strength. Radio transmitters, receivers and computers were used in a laboratory to measure signal level transmitted through six different roofing materials at a frequency of 9.4GHz. Decra offered the highest attenuation whereby 90% of the signal propagated was lost, out of which 60% was due to reflection. The equivalent transmission path field strength was 57dBmV/M against an International Civil Aviation Organization (ICAO) recommended minimum specification of minus 28dBmV/M. Similarly decra exhibited desired-to-undesired signal ratio of minus 16dB against ICAO recommended value of 20dB. Highest and lowest reflections occurred at angles of incidence of 90 and 135 degrees respectively. Generally roofing materials had little effect on nav aids signal strength in the transmission paths but had significant effect in the reflection paths. Highly reflective roofing materials such as steel and decra are not recommended for use in aerodrome areas. Based on these findings, building industry and flight navigation authorities have been challenged to develop a compromise roofing material.

**Keywords:** Interference, Nav aids, Propagation, Signal strength, Aerodrome

## 1. Introduction

Obstacles that affect radio navigation aid systems (nav aids) are structures in the vicinity of airport flight path. Reflections from these obstacles may interfere with direct radiating beam from the Instrument Landing System (ILS) and cause the course line to deviate from a straight line. Any large reflecting objects within the radiated signal area have the potential to cause multipath interference to the ILS signal source and path structure (Cortesi et al., 2002; Marcum, 2002).

A previous study by Keabajian (2008) showed that 51% of air accidents occur during final approach and landing (refer to Fig.1.). It was observed that flights maximize usage of nav aids in the final stretch. However no data was availed to determine the contribution of nav aids to the accidents. Therefore the effect of buildings on propagation of nav aids signal was not factored in the analysis.

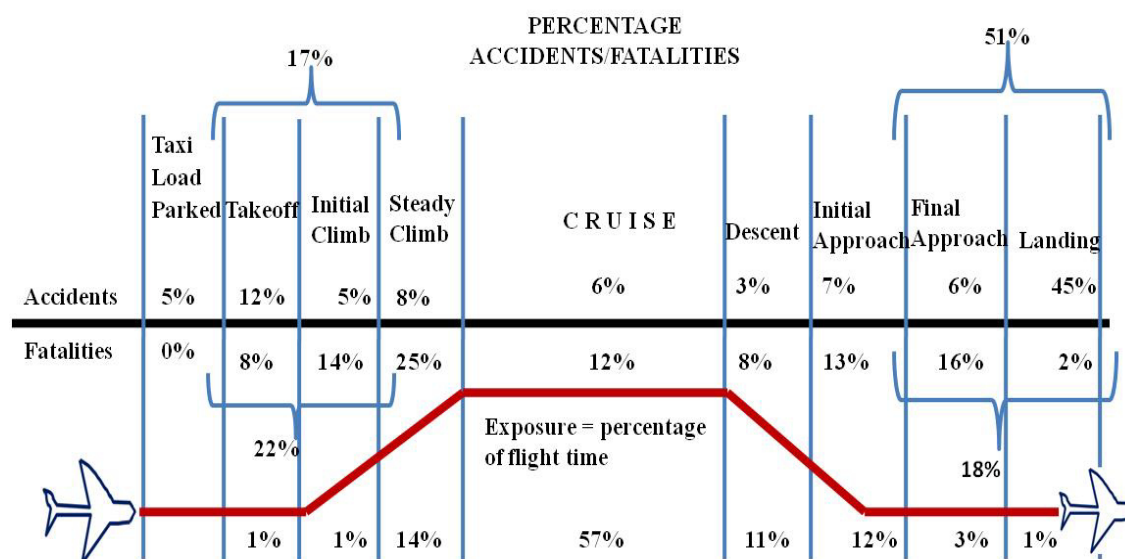


Figure 1. Relationship of flight sector and accidents (Kebabjian, 2008)

Chomba et al., (2011a), Marcum (2002) and Cortesi et al., (2002) also conducted a study on the effects of some of these obstacles on microwave signal transmission but very little was done to investigate effects of particular obstacles on nav aids signal strength. This paper aimed at investigating the behaviour of radio navigation signals when subjected to obstacles made of aluminum, iron, steel, clay, decra and plastic.

### 1.1 Empirical Underpinning

Buildings distort nav aids signals between the aircraft and ground equipment thus risking loss of intelligence in transmissions. Such interference could have devastating effects on flight navigation especially during landing. These structures around airports have been restricted partly because they pose a technical threat to flight navigation. This restriction is not supported by sufficient data concerning the influence of roofing materials on radio navigation signal.

### 1.2 Paper justification

With controlled heights of structures around the aerodromes, roofing materials were considered to be the most significant sources of interference to navigation signal since they are more exposed (Biermann et al., 2008). Comprehensive data on propagation of air navigation signals through roofing materials has been lacking. Therefore this paper attempts to generate data on roofing materials based on their effects on nav aids signal strength.

### 1.3 Scope and limitations

Friis' formula of free space loss showed that propagation loss at 9.4GHz was 112dB per km. The study represented a field environment scaled down to a laboratory environment using Fraunhofer distance equation (Balanis, 2005; Volakis, 2007). Fraunhofer's equation based on 9.4GHz and 16mm dipole antenna enabled a distance of 100cm to fulfill far-field conditions that are equivalent to open field environment. International Civil Aviation Organization (ICAO) has standardized and recommended minimum received signal strength in nav aids designated operation area as minus 28dBmV/M. Whereas atmospheric conditions in the field are dynamic and bound to affect the propagation of nav aids signals, the environment in the laboratory was assumed to be constant. The effects of snow, clouds, rain, reflective ground and masses of water on nav aids signals have been studied (Shah et al., 2008; Marcum, 2008; Tromboni, 2010; Biermann et al., 2008; Hueschen et al., 1994).

### 1.4 Interaction of obstacles and radio navigation signals

Attenuation is the reduction of signal strength during transmission. It may be due to free-space loss, scattering, refraction, diffraction, reflection, multipath, and absorption (see Fig. 2). Attenuation is also influenced by terrain contours, environment, propagation medium, the distance between the transmitter and the receiver, and the

height and location of antennas. Navigation signals scatter when they encounter obstacles in the line of sight. Scattering of the signal occurs when there are objects of comparable dimensions to the wavelength of the radiation in the medium of transmission. Scattering is particularly prevalent when there are rough and irregular surfaces present (Gupta, 2005; Kopp, 2000).

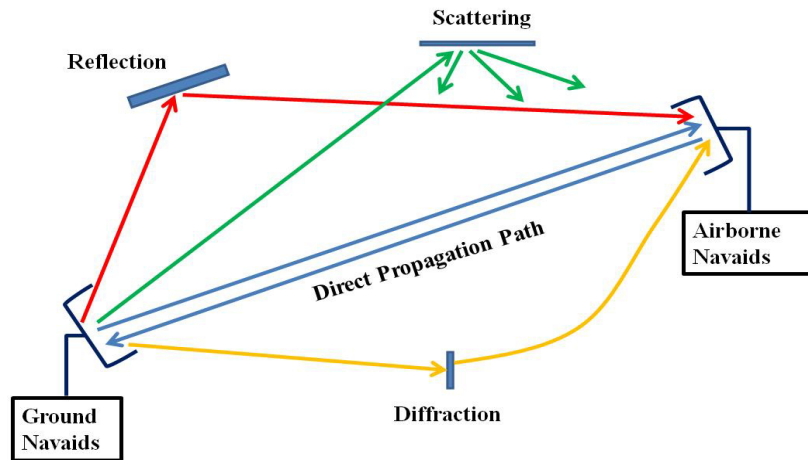


Figure 2: Effects of Obstacles and Multipath Propagation of Navaid Signals

The RF signals emitted by antenna go through significant attenuation, even in free space before they reach intended recipient. The free space propagation loss is given by Eq.1.1 (Debus, 2005; Tsai, 2011).

$$L(dB) = 32.5 + 20 \text{Log}F + 10 n \text{Log}D \tag{1.1}$$

F is transmission frequency in MHz  
 D is distance in kilometers  
 n is path loss exponent

Reflection of signal rays on material surfaces is significant in radio transmissions. Fig. 3 shows the relationships.

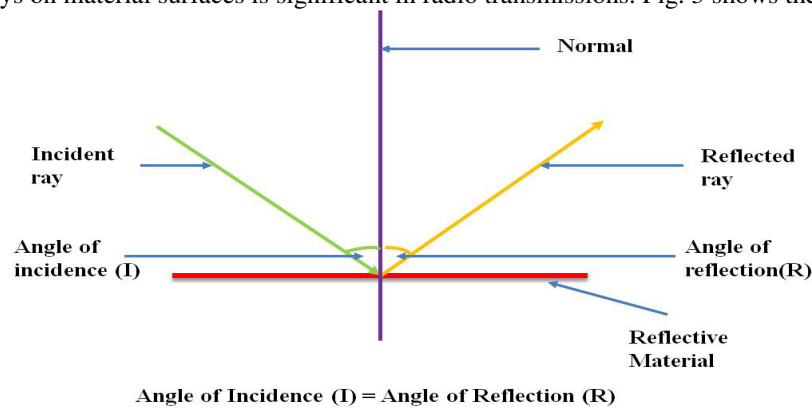


Figure 3: Relationship between angle of incidence and angle of reflection

Eq.1.2 represents empirical formula for electric field strength distribution for radiation patterns of dipole antennas of given electrical lengths (Briendenbach & Kloza, 2007)

$$e = E \cdot \left| \frac{\cos\left(\frac{\pi l_{el}}{\lambda_o}\right) \sin(\varphi + \varphi_o) - \cos\left(\frac{\pi l_{el}}{\lambda_o}\right)}{\cos(\varphi + \varphi_o)} \right| \quad (1.2)$$

Where

e = electric field strength distribution

E = amplitude of field strength

$l_{el}$  = electrical length

$\lambda_o$  = free space wavelength

$\varphi$  = polar angle

$\varphi_o$  = reference angle

The near-field and far-field are regions of electromagnetic field around an object such as transmitting antennas. The near-field strength decreases with distance, whereas far-field strength decreases with the inverse square of distance (Balanis, 2005). The boundary between the two regions depends on the dominant wavelength emitted by the source (Volakis, 2007).

Far-field carries a relatively uniform wave pattern, the far-field energy escapes to infinite distance. Near-field refers to regions such as near conductors and inside polarized media where propagation of electromagnetic waves is interfered with. The interaction with the media can cause energy to deflect back to source, in case of reactive near-field. The interaction with the medium can alternatively fail to return energy back to the source but cause a distortion in the electromagnetic wave (Rappaport, 2010). According to Woodhouse (2005) near-field is that part of the radiated field that is below distances shorter than the Fraunhofer distance as defined in Eq.1.3 and Fig. 4.

$$d \leq 2 \frac{D^2}{\lambda} \quad (1.3)$$

Where;

D = longitudinal antenna diameter of transmitting source.

$\lambda$  = wavelength

d = Fraunhofer distance

In both indoor and outdoor experiments, the distance between the source antenna and the receiver antenna must fulfill the far-field condition. Consequently a far field distance must be maintained as defined in Eq.1.4.

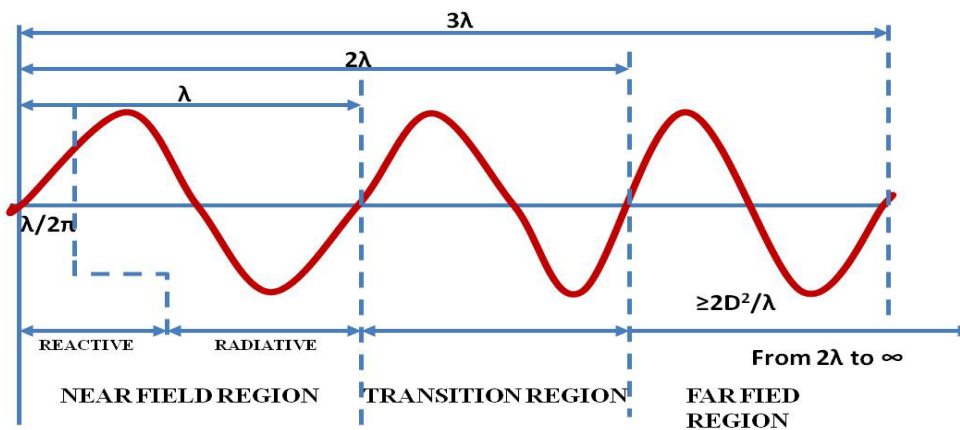
$$r_o \geq \frac{2(d_o + d_t)^2}{\lambda_o} \quad (1.4)$$

Where;

$r_o$  = distance between receiver and transmitter

$\lambda_o$  = wavelength of the radiated wave

$d_o$  and  $d_t$  = largest dimensions (in transverse or longitudinal direction) of the antenna



Note: Near Field:  $r \ll \lambda$ , Far Field:  $r \gg 2\lambda$

Figure 4: Near-field and far-field boundaries (Balanis, 2005)

Approach flight path is the designated path of an aircraft when approaching an aerodrome to enable safe expeditious maneuver before landing or taking off. This is the period and stretch within which the aircraft is nearing the airport zone boundary under the guidance of Air Traffic Control (ATC) and Nav aids. The civil aviation approach flight area covers approximately 7 by 7 square kilometers for international airports (Fig. 5). According to the convention of International Civil Aviation Organization ICAO (2009) that provides for aerodrome design and operations, buildings in this area are restricted. Constructions, dumping and farming are controlled. ICAO (2006) and ICAO (2001) provide procedures for air navigation services particularly on aircraft operations within aerodromes and flight paths including clearance for obstructions and air traffic management.

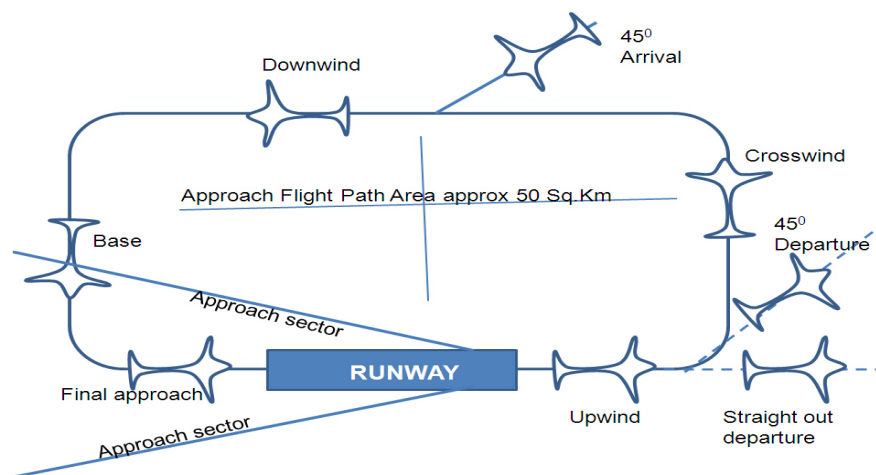


Figure 5: Typical approach flight path for an international airport

Extensive tests were conducted by the National Institute of Standards and Technology NIST (1997) to show how various common building materials can shield electromagnetic fields. A wide range of materials and thicknesses were tested, such as bricks, concrete, lumber, drywall, plywood, glass and rebar. Pauli and Moldon (2008) from University of Bundeswehr in Germany conducted similar study on additional building materials.

Just like this study, NIST (1997) and, Pauli and Moldon (2008) found that metals are far superior as shielding materials. Unfortunately, NIST did not test any roofing materials such as clay, decra, plastic, iron, steel or aluminum to determine their effects on radio signals. Marcum (2002) and Cortesi et al., (2002) conducted studies that dwelt on multipath errors caused by reflective and obstructive objects in the aerodrome. Singh (2003) and Briginton (2010) studied diffraction of microwaves while Gurung and Zhao (2007) examined attenuation.

## 2. Materials and Methods

### 2.1 Research site and instrumentation

East African School of Aviation laboratory for aeronautical telecommunications was the preferred site for this experiment. This laboratory is strategically designed and equipped to serve as a training, research and development centre for aeronautical telecommunications and avionics thus its choice. It is approved by ICAO as an aviation training organization for eastern and southern Africa. It is located next to Jomo Kenyatta International Airport in Nairobi.

The equipment and instruments for the study included the Gunn Oscillator whose purpose was to generate microwave frequency tuned at 9.4 GHz. This translates to a wavelength ( $\lambda$ ) of 32 mm and further translates to dipole aerial physical lengths of 8 mm ( $\lambda/4$ ) and 16 mm ( $\lambda/2$ ). These physical lengths were easily handled in a laboratory environment. Thus a choice of 9.4 GHz was the strategy to comfortably manage the experiment in a laboratory. A PIN modulator was used to modulate 10mW microwave signal before transmission. Also included was an 18dB gain horn antenna to radiate the microwave signals from the transmitter. A set of microwave absorbers were used to absorb stray microwave signals. The absorbers were placed around the equipment in an enclosure to shield against electromagnetic wave leakage.

Rotating antenna platform calibrated in polar deviations and designed for automatic rotation was used to enable a 360 degrees rotation. Different test antennas were mounted on this platform one at a time. Test antennas included dipole antennas whose characteristic impedance was 50 ohms. Dipole orientation was varied between vertical and horizontal polarization whereas helix antenna was used for circularly polarized waves. Two coaxial cables of two metres length and two stand rods of height 345mm were also used in the interconnect.

Personal Computer (PC) with Windows XP was loaded with CASSY LAB software to record and store radiation patterns, angular positions and signal levels in millivolts. A Coaxial detector in the receiver equipment was used to detect the microwave signal and provide equivalent dc for measurements. Sets of coaxial cables and microwave accessories were used to interconnect transmitter, receiver and PC as shown in Figures 6, 7 and 8. The computer screen display of Received Signal Level (RSL), angle of incidence and radiation pattern of dipole antenna are shown in Fig.9.

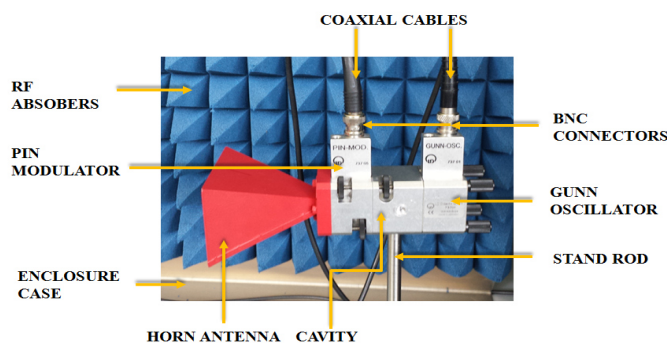


Figure 6: Transmitting Equipment Assembly

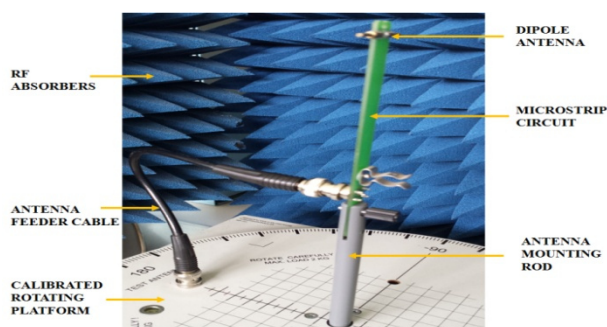


Figure 7: Receiving Equipment Assembly

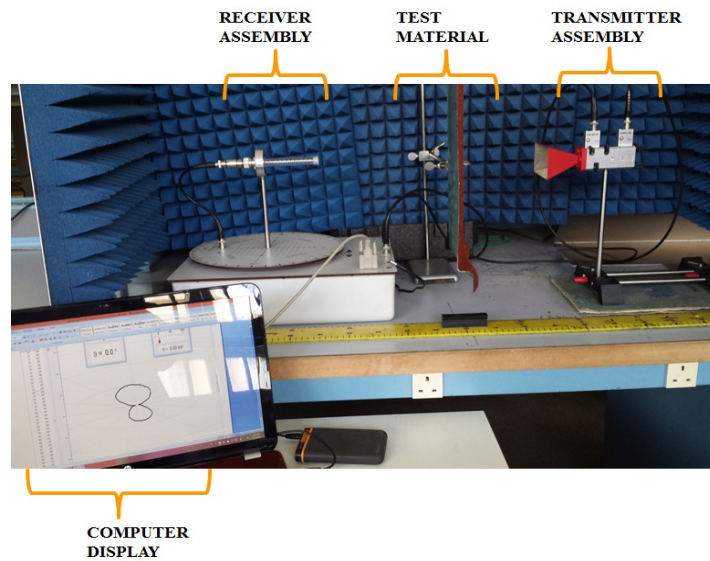


Figure 8: Interconnection of receiving and transmitting equipment

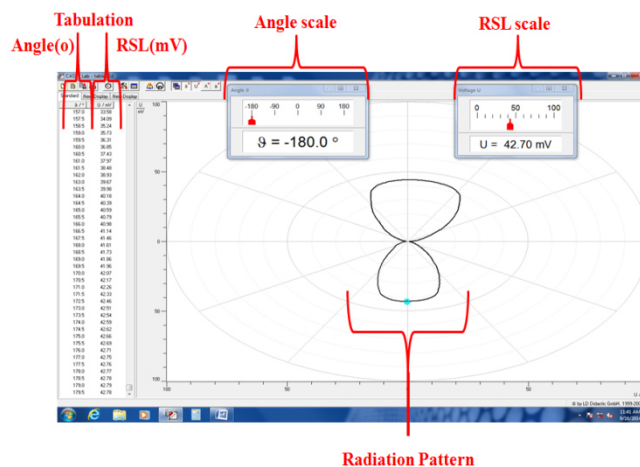


Figure 9: Computer screen print for horizontally oriented dipole antenna

### 2.2 Measurement and environmental control

The axis of symmetry of the test antenna and the centre of the rotary plate were put in line. The antenna was inserted in the central mounting of the rotary plate as a general fulfillment of a 360 degrees uniform motion. The main lobe of the test antenna was located at 0° in the directional diagram to enable its main-beam direction point into the 0° direction and aligned with the transmitting antenna. That meant that its back looked over to the exiting source antenna. The reason for this lies in the nature of the process that enables main-beam direction to be measured in one run instead of being divided into two halves. Environmental influences on the system thus have less effect on the important region of the main lobe (Briendenbach & Kloza, 2007).

The actual antenna signal  $A$  from the detector could not be measured directly. Only the voltage drop  $U$  generated by the detector current at the measuring amplifier was measurable. In general,  $U$  is not proportional to  $A$  but instead:

$$U \approx A^m \quad (2.1)$$

Where  $m$  describes the detector characteristics and depends on the power of incoming microwaves. In low power range  $m \approx 2$  so that  $U \approx A^2$ .

Preliminary experiments had shown that the assumed square behavior only applies at very low microwave powers or received voltages where  $U < 5$  mV. However, the antenna measurement system made it possible to enter other detector characteristics. The selected detector characteristics were checked and a variable attenuator was introduced which enabled the antenna signal in front of the detector to be attenuated in a well controlled way to handle voltage drops of up to 50mV.

### 2.3 Far-field and near-field condition tests

The test antenna was a dipole of half-wave length ( $\lambda/2$ ) which had a physical length of 16mm. The wavelength ( $\lambda_0$ ) of the radiated wave was 32mm. The mean distance between the source antenna and the test antenna was set at various distances i.e. 100cm, 60cm and 30cm. Maximum transverse measurement ( $d_0$ ) of radiating horn antenna was 100mm. Therefore the far field condition was checked by determining the minimum distance ( $r_o$ ) required to fulfill this condition given by Eq.1.4 so that  $r_o \geq 841$ mm. It was therefore shown that far-field conditions were fulfilled for test distance of 100cm.

However near-field conditions were tested for distances of 60cm and 30cm using the condition set by Equation 1.3 so that  $d \leq 625$ mm. It was shown that 30cm distance fulfilled near-field conditions. However 60cm distance was found to be at the boundary between near-field and far-field.

### 2.4 Measuring attenuation of received signal level at varying angles

The experiment was set up as in Fig. 8. Distance between the transmitter and the receiver was kept at 100 cm and the antenna orientation was maintained for horizontal polarization. The test materials were inserted one after the other at the center between the receiver and the transmitter. The material variation began from none, decra, aluminum, iron, clay, steel to plastic. The angle of incidence was varied from -180 degrees to +180 degrees at intervals of 0.5 degrees. For every material, three repetitions were performed and mean values noted. The propagated received signal levels (PRSL) were captured by the computer system and means recorded from 0 – 180 degrees in steps of 15 degrees.

### 2.5 Measuring reflected signal level at varying angles

The equipment was set up as in Fig. 10. The distance between the receiver and the test materials was kept at 100 cm. The receiver antenna orientation was maintained at Horizontal polarization. The transmitter was fixed at the Centre between the receiver and the test materials. The transmitter beam was focused to the test materials. The material variation began from Decra, Aluminum, Iron, Clay, steel to plastic. The angle of incidence was varied by automatic rotation of the receiver from -180 degrees to +180 degrees at intervals of 0.5 degrees. Reflections from the test materials were picked up by the receiver. For every material three repetitions were performed and mean values noted. The reflected received signal levels (RRSL) were captured by the computer system and means recorded from 0 – 180 degrees in steps of 15 degrees.

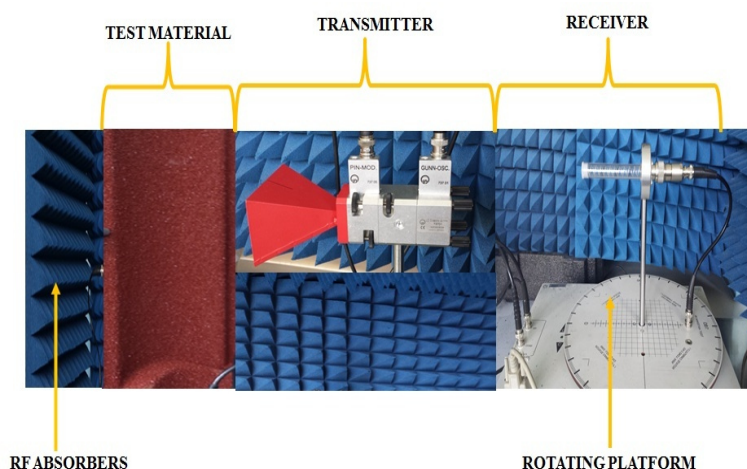


Figure 10: Measurement of reflected signal level



### 3. Results and Discussions

Table 1: Propagated Received Signal Levels (PRSL)

Propagated Received Signal Level in mV								
Distance (D) = 100 cm; Polarization = Horizontal								
Materials	None	Decra	Aluminum	Iron	Clay	Steel	Plastic	Mean
Angle(A°)								
0	8.08	0.10	2.39	4.69	4.72	1.21	4.91	3.73
15	6.60	0.09	2.50	3.91	3.93	0.88	3.70	3.01
30	3.88	0.12	1.94	2.52	2.87	0.16	1.55	1.86
45	1.37	0.12	1.30	1.39	1.19	0.40	0.25	0.86
60	0.67	0.09	0.59	0.64	0.67	0.24	0.04	0.42
75	0.32	0.07	0.20	0.30	0.51	0.06	0.02	0.21
90	0.08	0.05	0.11	0.32	0.30	0.02	0.09	0.14
105	0.41	0.03	0.03	0.42	0.13	0.09	0.37	0.21
120	1.02	0.06	0.00	0.61	0.17	0.22	0.78	0.49
135	2.54	0.01	0.08	0.96	0.52	0.53	1.67	0.90
150	4.80	0.12	0.45	2.41	1.36	0.98	3.07	1.88
165	7.63	0.11	1.10	3.30	2.98	1.55	4.74	3.06
180	7.63	0.06	1.54	3.62	3.42	1.32	4.86	3.21
Mean	3.46	0.08	0.94	1.93	1.75	0.59	2.00	

The propagated received signal level (PRSL) was converted to propagated received signal ratio (PRSR) by dividing PRSL by PRSL<sub>0</sub> at every angle of incidence for a given roofing material. Where PRSL<sub>0</sub> is the PRSL captured during none (no obstruction) measurement. PRSR values were recorded and plotted to generate Fig. 11

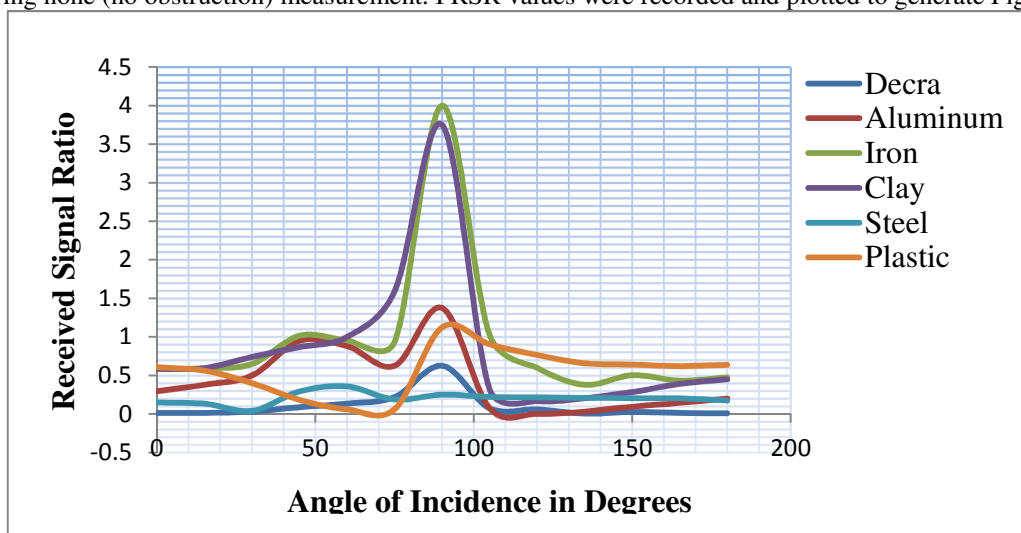


Figure 11: Variation of Propagated Received Signal Ratio (PRSR)

The PRSR was converted into Attenuated Signal Ratio (ASR) by formula;  $ASR = 1 - PRSR$ . ASR was converted to ASR (dB) by formula;  $ASR (dB) = 20 \log (ASR)$ . The results were recorded and plotted to generate Fig. 12.

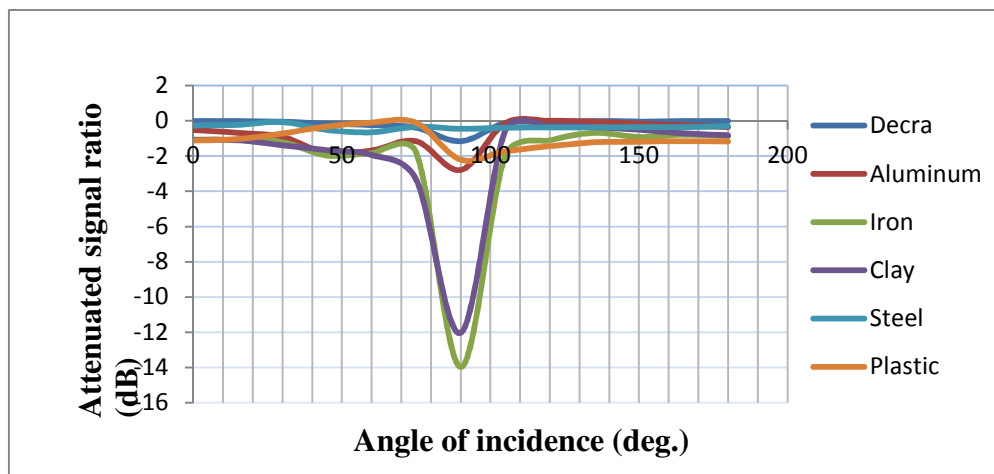


Figure 12: Variation of Attenuated Signal Ratio (ASR)

PPSR was converted to PRSR (dB) by formula;  $PRSR (dB) = 20 \log (PPSR)$ . The conversion to Received Signal Strength, RSS (dBm) was done by adding 30dB. The common impedance for aerial current was 50 ohms and therefore this was calculated by adding 47dB to RSS (dBm) to obtain RSS (dBmV/M) at a distance of one metre. Results were as recorded in Table 3.2.

Table 2. Propagated Received Signal Strength (RSS) per Material

Materials	PPSR	ASR	PRSR (dB)	ASR (dB)	RSS (dBm)	RSS (dBmV/M)
Decra	0.10	0.90	-20.0	-0.92	10.0	57.0
Steel	0.20	0.80	-14.0	-1.94	16.0	63.0
Aluminum	0.43	0.57	-7.30	-4.88	22.7	69.7
Plastic	0.56	0.44	-5.00	-7.13	25.0	72.0
Clay	0.84	0.16	-1.50	-15.9	28.5	75.5
Iron	0.93	0.07	-0.60	-23.1	29.4	76.4

Table 2 shows that decra offered the lowest propagation ratio (PPSR = 10% or -20dB) but presented the highest attenuation ratio (ASR = 90%). It therefore meant that decra offered the worst received signal strength (RSS = 57dBmV/M). Similarly the table shows that iron offered the highest propagation ratio (PPSR = 93% or -0.6dB) but presented the lowest attenuation ratio (ASR = 7%). It therefore meant that iron offered the best received signal strength (RSS = 76dBmV/M).

To compare attenuation in various roofing materials, data analysis was conducted using MS Excel data analysis tool kit. The test statistics applied were t-test and ANOVA single factor testing at 5% level of significance. Iron and clay exhibited different signal attenuation means, the test statistics showed that there was no significant difference between them and the two roofing materials showed the lowest attenuation effects. Aluminum and plastic exhibited medium signal attenuation means and the test statistics showed that they are similar. Decra and steel roofing materials are significantly similar yet different from the rest of the roofing materials. They exhibited the highest attenuation to the propagated signal. Table 3 shows the order of interaction.

Table 3. Interaction of received signal strength, materials and angle

Propagated Received Signal Strength RSS (dBmV/M)			
Materials	Mean	Max (90)	Min (135)
Decra	57.0	72.92	29.04
Steel	63.0	64.96	63.40
Aluminum	69.7	79.77	46.83
Plastic	72.0	78.02	73.35
Clay	75.5	88.48	63.24
Iron	76.4	89.04	68.48

The highest and lowest mean attenuation occurred at angles of incidence of 90 and 135 degrees respectively. The interactive tests showed that the lowest received signal strength (29dBmV/M) occurred on decra material at an angle of 135 degrees while the highest (89dBmV/M) occurred on iron at 90 degrees. The attenuation ratio decreased as the angle of incidence was varied from 0 degrees to 90 degrees.

Table 4: Reflected Received Signal Ratio (RRSR) in dB

Reflected Received Signal Ratio in dB								
Distance (D) = 100 cm; Polarization = Horizontal								
Materials	None	Decra	Aluminum	Iron	Clay	Steel	Plastic	Mean
<b>Angle(A°)</b>								
<b>0</b>	0.00	-3.70	-16.0	-25.0	-34.0	-9.30	-12.4	<b>-12.2</b>
<b>15</b>	0.00	-4.20	-14.6	-24.3	-28.4	-9.00	-11.8	<b>-12.0</b>
<b>30</b>	0.00	-4.90	-11.9	-20.6	-23.5	-7.90	-11.3	<b>-11.2</b>
<b>45</b>	0.00	-1.60	-6.50	-14.4	-13.8	-4.50	-7.30	<b>-6.80</b>
<b>60</b>	0.00	-2.00	-4.70	-12.4	-8.20	-4.50	-7.90	<b>-6.00</b>
<b>75</b>	0.00	-8.50	-0.30	-7.80	-6.60	-7.20	-10.1	<b>-6.10</b>
<b>90</b>	0.00	3.50	6.00	-1.20	0.00	9.50	-8.50	<b>3.30</b>
<b>105</b>	0.00	-3.60	-7.60	-20.2	-22.7	-0.90	-32.4	<b>-8.80</b>
<b>120</b>	0.00	-5.10	-21.1	-28.2	-34.0	-5.40	-19.3	<b>-12.9</b>
<b>135</b>	0.00	-7.70	-24.6	-35.9	-48.0	-11.2	-16.5	<b>-16.3</b>
<b>150</b>	0.00	-7.30	-18.1	-35.4	-48.0	-11.6	-15.1	<b>-15.4</b>
<b>165</b>	0.00	-7.90	-17.6	-33.2	-40.9	-12.2	-14.1	<b>-15.4</b>
<b>180</b>	0.00	-7.60	-17.4	-29.6	-35.9	-11.4	-12.7	<b>-14.7</b>
<b>Mean</b>		<b>-4.00</b>	<b>-7.4</b>	<b>-15.7</b>	<b>-15</b>	<b>-4</b>	<b>-12.3</b>	

Figure 13 is a chart generated from Table 4 and presents variation of reflection and angle of incidence for various roofing materials. The general pattern showed that each material exhibited angles of maximum and minimum reflection.

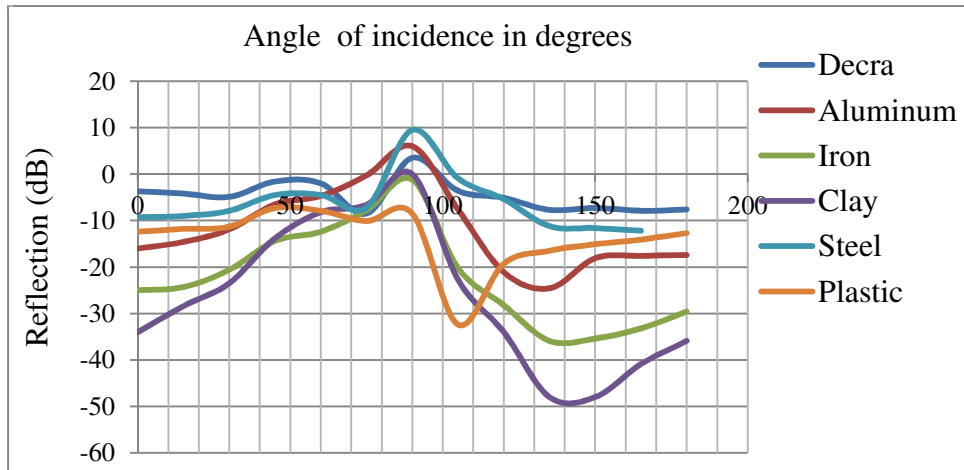


Figure 13: Variation of reflection and angle of incidence

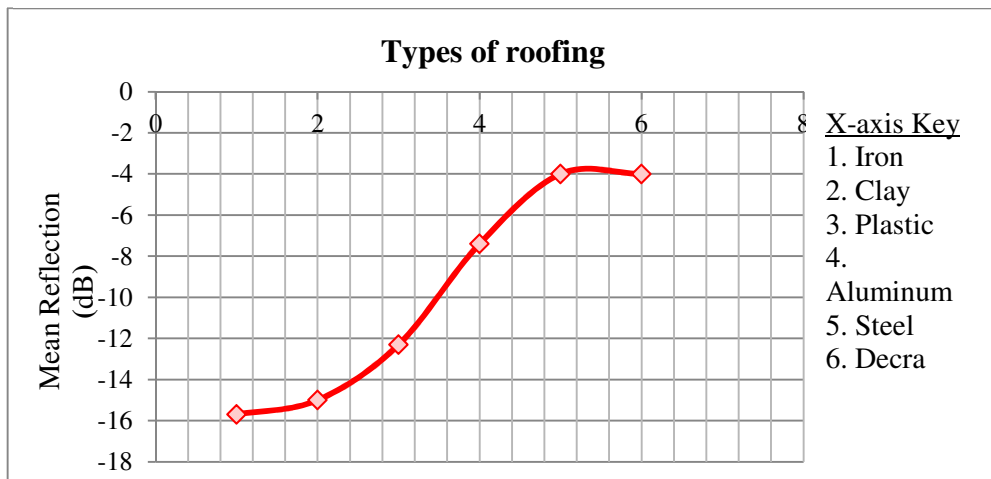


Figure 14: Variation of mean reflection across various materials

To compare reflection in various roofing materials, data analysis was conducted using MS Excel data analysis tool kit. The test statistic applied was t-test with a 5% level of significance. Whereas iron and clay exhibited different signal reflection means, the test statistics showed that there was no significant difference between them and the two roofing materials showed the lowest reflection effects. Aluminum and plastic exhibited medium signal reflection means and the test statistics showed that they are similar. Decra and steel roofing materials showed similar reflection effects. They exhibited the highest reflection of the propagated signal. Table 5 shows the order of interaction.

Table 5: Interaction of Reflected Received Signal Strength, material and angle

Reflected Received Signal Strength RSS (dBmV/M)			
Materials	Mean	Max (90)	Min (135)
Decra	73.01	80.52	69.32
Steel	73.03	86.54	65.82
Aluminum	69.65	83.02	52.42
Plastic	64.75	68.48	60.52
Clay	62.01	77.00	29.04
Iron	61.35	75.84	41.08

The highest and lowest mean reflection occurred at angles of incidence of 90 and 135 degrees respectively. The interactive tests showed that the lowest reflected signal strength (29dBmV/M) occurred on clay material at an angle of 135 degrees while the highest (86dBmV/M) occurred on iron at 90 degrees. Generally the reflected received signal ratio increased as angle of incidence varied from 0 degrees to 90 degrees across all materials.

The desired signal is one that reaches the receiver where it may be decoded. The undesired signal is one that is reflected and may indirectly reach the receiver or get lost. Decoding the undesired signal may introduce multipath errors in the measurement of distance and signal strength. International Civil Aviation Organization has specified that the minimum desired-to-undesired (D/U) signal ratio should be 20 dB (Kebabjian, 2008).

Table 6: Desired to Undesired Signal Ratio per a Material

Materials	Iron	Clay	Plastic	Aluminum	Steel	Decra
P-RSR	0.93	0.84	0.56	0.43	0.20	0.10
R-RSR	0.17	0.18	0.24	0.43	0.63	0.63
D/U ratio	5.47	4.67	2.33	1.00	0.32	0.16
D/U (dB)	14.8	13.4	7.35	0.00	-9.90	-15.9

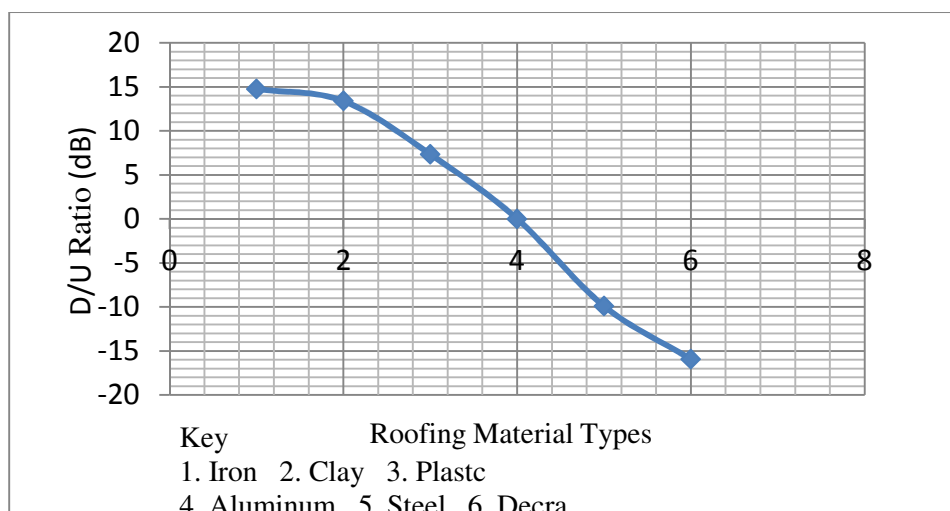


Figure 15: Variation of D/U signal ratio across material types

Figure 15 shows that Iron, clay and plastic have the highest D/U signal ratios but steel and decra have the lowest. The D/U signal ratio for aluminum is equal to 0 dB. This means that aluminum propagates and reflects signals in equal proportions. The D/U values for all the materials fall below the ICAO recommended value of 20dB.

#### 4. Conclusions and Recommendations

This paper sought to determine the effects of roofing materials on nav aids signal strength. Experiments were conducted at the East African School of Aviation in the aeronautical telecommunication laboratory. The analysis compared roofing materials by considering their effects on signal strength. The analysis revealed that roofing materials have little effect on nav aids signal strength in the transmission path. However the effects were very significant in the reflective path. The analysis found that highly reflective materials such as decra and steel have high attenuation. High reflection is a major source of interference in Nav aids signal transmission especially with the Distance Measuring Equipment where echoes create significant errors in measured distance (Andreassen, 2008).

Considering the transmission path, interaction between signal strength, materials and angle of incidence showed that decra inclined at an angle of 135 degrees offered the worst received signal strength (29dBmV/M). But iron material inclined at 90 degrees offered the best signal strength (89dBmV/M). ICAO recommends minimum signal strength of minus 28dBmV/M for designated operational coverage of nav aids (ICAO, 2010). It is therefore evident that in the transmission path, all the roofing materials in this study irrespective of the angle of inclination, showed significant effects on propagation of nav aids signal. However the affected signal strength remained above the recommended minimum.

But when reflection path was considered, the highest reflected signal strength was offered by steel (87dBmV/M) inclined at 90 degrees and the lowest was offered by clay (29 dBmV/M) inclined at 135 degrees. Recalling that reflection is a major cause of multipath interference, it is quite clear that the reflected signal which was way above the recommended minimum can find its way into the transmission path and cause significant interference on the forward signal strength (Selex, 2009). International Civil Aviation Organization has specified that the minimum Desired-to-Undesired (D/U) signal ratio should be 20 dB for air-ground communication systems (ICAO, 2012). All the roofing materials used in this study fall below this specification even though iron, clay and plastic have better values compared to aluminum, steel and decra. However aluminum exhibits unique characteristics whereby its D/U value is 0 dB. It means that aluminum propagates and reflects in equal proportions. It is also evident that the major component of the undesired signal is due to reflection. Compared to the recommended minimum D/U, it was established that roofing materials have significant effects on nav aids signal strength.

The findings of this study concur with Laws of Kenya Civil Airports Act CAP 395 (2005) and Civil Aviation Act No. 21 (2013) on restriction of structures around designated operational areas of aerodromes and flight paths. It also concurs with ICAO (2009) on civil aviation security regulations for protection of airports, aircrafts and navigation facilities. This concurrency means that highly reflective roofing materials are significant hazards to air transport. This paper recommends that building and avionics industries develop a compromise roofing material that has little effect on flight navigation. Similarly the angle at which roofs are inclined should be designed to minimize reflections as per the data provided in this research. Further studies should be conducted in open field environment where sources of variability such as weather conditions can be factored in the experimental design.

## References

- Andreassen, S. O. (2008). *Principles of enroute navigation systems*. Norwegian Telecommunication Administration, Oslo
- Balanis, C. A. (2005). *Antenna theory: Analysis and Design*. Prentice Hall Inc. 3<sup>rd</sup> Ed. Ch 2, p. 34.
- Biermann, W. D., Greving, G., & Mundt, R. (2008). *Status of advanced scattering distortion: system analysis for Nav aids and radar- examples of A380 and windturbines*. Microwave radar and remote sensing symposium, September 22-24, 2008, pp. 42-47. Retrieved from [www.researchgate.net](http://www.researchgate.net). Accessed on 23<sup>rd</sup> May 2012
- Briendenbach, K., & Kloza, J. M. (2007). *Antenna technology*. Huerth: LD Didactic GmbH.
- Briginton, M. (2010). *Microwave transmission through a metal capped array of holes in metal sheet*. University of Exeter. UK.
- Chomba, B. K., Konditi, D.B.O., Nyaanga, D. M., & Githeko, J. M. (2011a). Effects of varying angle of incidence on wireless signal propagation, *International Journal of Pure and Applied Science and Technology*, 7, (1), pp.22 -29. [www.ijopaasat.in](http://www.ijopaasat.in)
- Cortesi, N., Ducci, M., Nobiletti, A., & Parente, A. (2002). *The mixed use of flight inspection and computer simulation: the ENAV experiences with AIRNAS*. 12<sup>th</sup> international flight inspection symposium, Rome: international committee for aerospace standards and calibration, Doc No. 22. Retrieved from [www.icasc.co](http://www.icasc.co). Accessed on 24<sup>th</sup> May 2012.
- Debus, W. (2005). *RF path loss and transmission distance calculations*. Technical Memorandum, August 4, pp 1- 12, Axionn, LLC. Retrieved from [www.sciepub.com](http://www.sciepub.com). Accessed on 25<sup>th</sup> March 2015.
- Gupta, D. (2005). *WLAN signal characteristics in an indoor environment-an analytic model and experiments*, University of Maryland, College Park.
- Gurung, S., & Zhao J. (2007). *Attenuation of microwave signals and its impacts on communication systems*. University of North Texas. Department of electrical engineering. Retrieved from [www.sanjaygurung.com](http://www.sanjaygurung.com). Accessed on 17<sup>th</sup> May 2012.

- Hueschen, R. M., & Knox C. E. (1994). *Modeling of ILS localizer signal on runway 25L at Los Angeles international airport*. Virginia: Langley Research Centre, National Aeronautics and Space Administration. NASA Technical Memorandum 4588
- International Civil Aviation Organisation (ICAO) (2006) *Procedures for air navigation services and aircraft operations*. Doc 8168 Vol. 1-4, Montreal, ICAO
- International Civil Aviation Organization (ICAO) (2001). *Air Traffic services*, Annex 11 Vol.1-2, Montreal, ICAO
- International Civil Aviation Organization (ICAO) (2010). *Manual on testing of radio navigational aids*; Doc 8071, Vol.1-3. Montreal, ICAO
- International Civil Aviation Organization (ICAO) (2009). *Aerodrome designs and operations*, Annex 14 Vol.1, Ch.14, Montreal, ICAO
- International Civil Aviation Organization (ICAO) (2012). *Handout on radio frequency spectrum requirements for civil aviation; assignment planning criteria for radio communication and navigation systems* Doc 9718 Vol.2, Montreal, ICAO
- Kebabjian, R. (2008). *OAGback aviation solutions 1988-2007*. Retrieved from [www.planecrashinfo.com](http://www.planecrashinfo.com). Accessed on 15<sup>th</sup> September, 2010
- Kopp, C. (2000). *Microwave and milimetric wave propagation*. Retrieved from [www.ausairpower.net](http://www.ausairpower.net). Accessed on 20<sup>th</sup> November, 2010
- Laws of Kenya, Civil Aviation Act No. 21 (2013). *Prohibitions and Control of structures around aerodromes*, Parts II (40), V (56) and V (57) Nairobi, Government printers, July 2013.
- Laws of Kenya, Civil Airports Act CAP 395. (2005). *Regulating buildings and other structures around airports*. Nairobi. Government Printer.
- Marcum, F. (2008). Analysis of instrument landing system glide slope performance sensitivity to sideband-only phase variances. *The institute of navigation*, 47 (4) pp. 239-244.
- Marcum, F. (2002). *Design of an image radiation monitor for instrument landing system glide slope*. IEEE transactions on aerospace and electronic systems, DOI 10.1109/7.705891.
- National Institute of Standards and Technology, (1997). *EMF shielding by building materials; Attenuation of microwave band electromagnetic fields by common building materials*, NIST. USA
- Pauli, P., & Moldon D. (2008). *EMF shielding by building materials; Attenuation of microwave band electromagnetic fields by common building materials*, NIST. USA. Press/Prentice Hall PTR, Upper Saddle River, New Jersey.
- Rappaport, T. S. (2010). *Wireless communication principles and practice* 2<sup>nd</sup> Ed. Prentice Hall Inc. 19<sup>th</sup> Printing, p.108.
- Selex Inc. (2009). *Technical manual for maintenance of Doppler VHF Omnidirectional Range*, Selex Milan.
- Shah, A. P., Pritchett, A. R., Feigh, A. M., & Kalaver, S. A. (2008). *Analyzing air traffic management systems using agent based modeling and simulation*. Atlanta GA: Georgia Institute of Technology
- Singh, R. (2003). *Microwave diffraction and interference*. Ryerson University. Retrieved from [www.stw.ryerson.ca](http://www.stw.ryerson.ca). Accessed on 16<sup>th</sup> February, 2011
- Tromboni, P. D., & Palmerin, G. B. (2010). Navigational aids performance evaluation for precision approaches. Rome: *International Journal of Aerospace Engineering*, doi:10.1155/2010/389832
- Tsai, M. (2011). *Path-loss and Shadowing (Large-scale Fading)*; National Taiwan University October 20, 2011.
- Volakis, J. L. (2007). *Antenna engineering handbook*, 4<sup>th</sup> Ed. Mc Graw-Hill Retrieved from <https://m.electronicdesign.com> June 8, 2012.
- Woodhouse, I. H. (2005). *Introduction to microwave remote sensing: how to replicate FF conditions before launch to provide an accurate calibration of antenna that can replicate FF conditions*. Retrieved from <https://books.google.com>

The IISTE is a pioneer in the Open-Access hosting service and academic event management. The aim of the firm is Accelerating Global Knowledge Sharing.

More information about the firm can be found on the homepage:

<http://www.iiste.org>

### CALL FOR JOURNAL PAPERS

There are more than 30 peer-reviewed academic journals hosted under the hosting platform.

**Prospective authors of journals can find the submission instruction on the following page:** <http://www.iiste.org/journals/> All the journals articles are available online to the readers all over the world without financial, legal, or technical barriers other than those inseparable from gaining access to the internet itself. Paper version of the journals is also available upon request of readers and authors.

### MORE RESOURCES

Book publication information: <http://www.iiste.org/book/>

Academic conference: <http://www.iiste.org/conference/upcoming-conferences-call-for-paper/>

### IISTE Knowledge Sharing Partners

EBSCO, Index Copernicus, Ulrich's Periodicals Directory, JournalTOCS, PKP Open Archives Harvester, Bielefeld Academic Search Engine, Elektronische Zeitschriftenbibliothek EZB, Open J-Gate, OCLC WorldCat, Universe Digital Library, NewJour, Google Scholar

